

# PREDICTIVE CONTROL OF STRUCTURES

By José Rodellar,<sup>1</sup> Alex H. Barbat,<sup>2</sup> and Juan M. Martín-Sánchez<sup>3</sup>

**ABSTRACT:** Different continuous-time approaches have been proposed in recent years to formulate active control algorithms to reduce the response of civil engineering structures under dynamic excitations. In this paper, a general formulation of a new discrete-time control methodology is presented and applied to structural control. This methodology, based on the concept of predictive control, is discussed and compared to the optimal control methodology by means of numerical examples.

## INTRODUCTION

The impact of control theory in the different domains of engineering and applied sciences has become increasingly important in the last few decades. Although the body of this theory is extremely broad and rich, it has essentially been built up on a few basic control strategies. Negative feedback, a strategy of remarkable simplicity that computes the control signal by using the difference between the set point and the process output, was the first strategy to be considered and the one most used in practical applications. In an attempt to improve the performance of negative feedback systems, a more sophisticated control strategy, optimal control, was developed. According to the concepts of optimal control, the control signal is calculated by minimizing a performance index that requires the solution of a Riccati equation (Bryson and Ho 1975; Sage and White 1977). Pole placement was another strategy to be considered, based on the assignment of specific values to the closed-loop poles (Brogan 1974).

The introduction of digital computers in control systems motivated not only the discrete-time formulation of the aforementioned control strategies, first formulated in continuous-time, but also the development of new digital control strategies. Predictive control was developed within this context as a control strategy that computes the control signal which makes the predicted process output equal to a desired process output. This desired output belongs to a desired output trajectory generated by a driver block. The predictive control strategy was first defined within a more general adaptive-predictive control system (APCS) introduced by Martín-Sánchez (1974; 1976a; 1976b) and used in a number of control applications (Martín-Sánchez 1977; Martín-Sánchez and Shah 1984).

The interest in reducing the response of structures subjected to dynamic excitations produced by earthquakes, wind, moving loads, and others has led to the use of control techniques in this field as well (Yao

<sup>1</sup>Assoc. Prof., School of Civ. Engrg., Tech. Univ. of Catalunya, Jordi Girona 31, 08034, Barcelona, Spain.

<sup>2</sup>Visiting Prof., School of Civ. Engrg., Tech. Univ. of Catalunya, Barcelona, Spain.

<sup>3</sup>Assoc. Prof., School of Mineral Engrg., Tech. Univ. of Madrid, Madrid, Spain.

Note.—Discussion open until November 1, 1987. To extend the closing date one month, a written request must be filed with the ASCE Manager of Journals. The manuscript for this paper was submitted for review and possible publication on May 12, 1986. This paper is part of the *Journal of Engineering Mechanics*, Vol. 113, No. 6, June, 1987. ©ASCE, ISSN 0733-9399/87/0006-0797/\$01.00. Paper No. 21538.

1972). In order to develop active structural control systems, different methods have been taken from control theory in recent years. Thus, some works have been based on the negative feedback strategy (Yang and Giannopoulos 1978; Roorda 1980), others have used the pole placement approach (Martin and Soong 1976; Abdel-Rohman and Leipholz 1978), but the most widely used technique has been optimal control as considered in Yang (1975), Abdel-Rohman and Leipholz (1979), Chang and Soong (1980), and Meirovitch and Silverberg (1983). Recently, predictive control schemes have also been applied to structural control (Rodellar and Barbat 1985a; 1985b; Rodellar and Martín-Sánchez 1986).

In this paper a general formulation of predictive control is presented, based on a general driver block design as proposed in Martín-Sánchez (1980) and Rodellar (1982). This design essentially consists of generating a desired output trajectory that satisfies a certain performance criterion. Distinct solutions for the driver block can be found depending on the criterion chosen. Two solutions are included in this paper. One of these minimizes a linear quadratic index, thus requiring the solution of a Riccati equation. Within this case, a standard optimal control problem may be formulated. The other does not require a Riccati equation and is therefore more attractive. Practical examples in the field of structural control are presented and used to compare the predictive control approach with that of optimal control.

Previous approaches for structural control have been formulated in continuous-time, thus requiring an "a posteriori" discretization of the control law for computer implementation. Conversely, in this paper a discrete-time representation of the structural control problem is given, which allows the direct application of the predictive control strategy within a digital control scheme.

## GENERAL FORMULATION OF PREDICTIVE CONTROL

In order to implement the predictive control strategy, the block diagram shown in Fig. 1, which includes a predictive model and a driver block, can be considered. The predictive model is used at each sampling instant to compute the control signal which makes the predicted process output belong to a desired output trajectory. The driver block is designed to generate a desired output trajectory that satisfies a performance criterion.

In the driver block design, an interval  $[k, k + \lambda]$  is considered at each sampling instant  $k$ , and the predictive model is used to predict a process

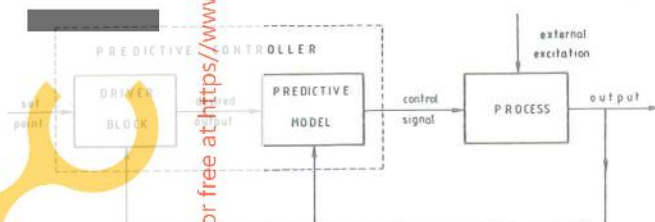


FIG. 1—Basic Scheme of Predictive Controller

output sequence as a function of a control sequence. The predictive model can be formulated by means of a discrete-time state model of the form

$$\hat{\mathbf{x}}(k + j|k) = \mathbf{A}\hat{\mathbf{x}}(k + j - 1|k) + \mathbf{B}\hat{\mathbf{u}}(k + j - 1|k) \dots\dots\dots (1a)$$

$$\hat{\mathbf{y}}(k + j|k) = \mathbf{H}\hat{\mathbf{x}}(k + j|k) \dots\dots\dots (1b)$$

where  $\hat{\mathbf{x}}(k + j|k)$  and  $\hat{\mathbf{y}}(k + j|k)$  = the state vector and the process output predicted at instant  $k$  for the instant  $k + j$ , respectively;  $\hat{\mathbf{u}}(k + j|k)$  = the control sequence; and  $\mathbf{A}$ ,  $\mathbf{B}$ , and  $\mathbf{H}$  = the discrete-time system matrix, control matrix, and output matrix, respectively.

This model is redefined at each instant  $k$  in the form

$$\hat{\mathbf{x}}(k|k) = \mathbf{x}(k); \quad \hat{\mathbf{u}}(k|k) = \mathbf{u}(k) \dots\dots\dots (2)$$

where  $\mathbf{x}(k)$  and  $\mathbf{u}(k)$  = the state vector and the control signal at instant  $k$ , respectively.

Matrices  $\mathbf{A}$  and  $\mathbf{B}$  in Eq. 1a are here considered to be known and constant. In a more general adaptive-predictive control system, these matrices are time-dependent and are updated at each sampling instant  $k$  by means of estimation algorithms (Martín-Sánchez 1980; Martín-Sánchez and Shah 1984).

The driver block under its general design selects at each instant  $k$ , as desired output trajectory  $\mathbf{y}_d$ , the process output sequence in the finite interval  $[k + 1, k + \lambda]$  which is caused, according to the predictive model, by a control sequence in the interval  $[k, k + \lambda - 1]$  in such a way that both sequences satisfy a certain performance criterion. This performance criterion may be formulated by means of an index that may include, in a general case, the predicted output and the control sequences as well as a reference trajectory.

Two different solutions for the driver block design problem are presented in the following sections. In the first one a linear quadratic index is minimized by solving a Riccati equation. In order to obtain a more economic solution, the second one considers the minimization of an index in which a specific shape for the control sequence is imposed.

### DRIVER BLOCK SOLUTION VIA RICCATI EQUATION

The driver block performance index may be defined by the following linear quadratic cost function:

$$J = \frac{1}{2} \sum_{j=0}^{\lambda} [\hat{\mathbf{y}}(k + j|k) - \mathbf{y}_r(k + j)]^T \mathbf{Q}(j) [\hat{\mathbf{y}}(k + j|k) - \mathbf{y}_r(k + j)] + \frac{1}{2} \sum_{j=0}^{\lambda-1} \hat{\mathbf{u}}(k + j|k)^T \mathbf{R}(j) \hat{\mathbf{u}}(k + j|k) \dots\dots\dots (3)$$

where the weighting matrices  $\mathbf{Q}(j)$  ( $j = 0, 1, \dots, \lambda$ ) and  $\mathbf{R}(j)$  ( $j = 0, 1, \dots, \lambda - 1$ ) are real positive semidefinite, and  $\mathbf{R}(j)$  are also nonsingular. The reference trajectory  $\mathbf{y}_r$  may be redefined at each sampling instant  $k$  starting from the current output and evolving towards the setpoint according to a chosen dynamics.

Following standard optimization procedures (Sage and White 1977), the minimization of index  $J$  introduces a  $2n \times 2n$  matrix  $\mathbf{P}(k)$  that satisfies

a discrete-time matrix Riccati equation of the form

$$\mathbf{P}(k+j) = \mathbf{H}^T \mathbf{Q}(j) \mathbf{H} + \mathbf{A}^T \mathbf{P}(k+j+1) [\mathbf{I} + \mathbf{B} \mathbf{R}^{-1}(j) \mathbf{B}^T \mathbf{P}(k+j+1)]^{-1} \mathbf{A};$$

$$j = 0, 1, \dots, \lambda \dots \dots \dots (4a)$$

$$\mathbf{P}(k+\lambda) = \mathbf{H}^T \mathbf{Q}(\lambda) \mathbf{H} \dots \dots \dots (4b)$$

and a  $2n$  vector  $\boldsymbol{\eta}(k)$  that satisfies the equation

$$\boldsymbol{\eta}(k+j) = \mathbf{H}^T \mathbf{Q}(j) \mathbf{y}_r(k+j) + \mathbf{A}^T \boldsymbol{\eta}(k+j+1) - \mathbf{A}^T \mathbf{P}(k+j+1)$$

$$[\mathbf{I} + \mathbf{B} \mathbf{R}^{-1}(j) \mathbf{B}^T \mathbf{P}(k+j+1)]^{-1} \mathbf{B} \mathbf{R}(j)^{-1} \mathbf{B}^T \boldsymbol{\eta}(k+j+1);$$

$$j = 0, 1, \dots, \lambda \dots \dots \dots (5a)$$

$$\boldsymbol{\eta}(k+\lambda) = \mathbf{H}^T \mathbf{Q}(\lambda) \mathbf{y}_r(k+\lambda) \dots \dots \dots (5b)$$

Then the sequence of vectors in  $[k, k+\lambda-1]$  that minimizes the index is expressed as:

$$\hat{\mathbf{x}}(k+j|k) = -\mathbf{D}(k+j) \hat{\mathbf{x}}(k|k) + \mathbf{u}_0(k+j) \dots \dots \dots (6)$$

where  $\mathbf{D}(k+j)$  is an  $r \times 2n$  gain matrix expressed as

$$\mathbf{D}(k+j) = \mathbf{R}^{-1}(j) \mathbf{B}^T (\mathbf{A}^T)^{-1} [\mathbf{P}(k+j) - \mathbf{H}^T \mathbf{Q}(j) \mathbf{H}] \dots \dots \dots (7)$$

and  $\mathbf{u}_0(k+j)$  is an  $r$  vector given by

$$\mathbf{u}_0(k+j) = \mathbf{R}^{-1}(j) \mathbf{B}^T (\mathbf{A}^T)^{-1} [\boldsymbol{\eta}(k+j) - \mathbf{H}^T \mathbf{Q}(j) \mathbf{y}_r(k+j)] \dots \dots \dots (8)$$

According to the driver block design, the control vector  $\mathbf{u}(k)$  to be applied at instant  $k$  is, as indicated in Eq. 2, the value at instant  $k$  of the input sequence given by Eq. 6. Then, by making  $j = 0$  in Eq. 6 and taking into account the definition at instant  $k$  of the predicted state  $[\hat{\mathbf{x}}(k|k) = \mathbf{x}(k)]$ , one obtains the following control law:

$$\mathbf{u}(k) = -\mathbf{D}(k) \mathbf{x}(k) + \mathbf{u}_0(k) \dots \dots \dots (9)$$

In order to obtain the gain matrix  $\mathbf{D}(k)$  and the vector  $\mathbf{u}_0(k)$ , Eqs. 4a and 5a must be solved recursively backwards in time starting from the terminal conditions 4b and 5b for  $j = \lambda$  to  $j = 0$ , and then Eqs. 7 and 8 must be applied for  $j = 0$ .

This formulation of the driver block design essentially differs from the standard optimal control problem in the sense that the optimization procedure is repeated at each sampling instant  $k$ , since the prediction horizon is redefined, which is inherent in the predictive control strategy. As is well known, in optimal control the optimization problem is solved only once at the initial instant  $k = 0$ . Thus, if in Eqs. 4–8 one makes  $k = 0$  and  $\lambda = N$ , where  $N$  is the final instant of the control action, an optimal control formulation is found. By way of example, in the optimal regulator problem, which corresponds to a null reference trajectory  $\mathbf{y}_r$ , a Riccati equation of the form

$$\mathbf{P}(j) = \mathbf{H}^T \mathbf{Q}(j) \mathbf{H} + \mathbf{A}^T \mathbf{P}(j+1) [\mathbf{I} + \mathbf{B}^{-1} \mathbf{R}(j) \mathbf{B}^T \mathbf{P}(j+1)]^{-1} \mathbf{A};$$

$$j = 0, 1, \dots, N \dots \dots \dots (10a)$$

$$\mathbf{P}(N) = \mathbf{H}^T \mathbf{Q}(N) \mathbf{H} \dots \dots \dots (10b)$$

must be solved. In this case  $\mathbf{u}_0$  is a null vector and the gain matrix is given by

$$\mathbf{D}(j) = \mathbf{R}^{-1}(j)\mathbf{B}^T(\mathbf{A}^T)^{-1}[\mathbf{P}(j) - \mathbf{H}^T\mathbf{Q}(j)\mathbf{H}] \dots \dots \dots (11)$$

and the control law is

$$\mathbf{u}(j) = -\mathbf{D}(j)\mathbf{x}(j) \dots \dots \dots (12)$$

**DRIVER BLOCK SOLUTION VIA SHAPED CONTROL SEQUENCES**

The driver block performance criterion may consist of the minimization of an index in which the control sequence has a specified shape on the prediction horizon. Particular choices of the shape of the control sequence may be that of a step or of a pulse. One may consider, as an example, the following index:

$$J = \frac{1}{2} \sum_{j=1}^{\lambda} [\hat{\mathbf{y}}(k+j|k) - \mathbf{y}_r(k+j)]^T \mathbf{Q}(j) [\hat{\mathbf{y}}(k+j|k) - \mathbf{y}_r(k+j)] + \frac{1}{2} \hat{\mathbf{u}}(k|k)^T \mathbf{R} \hat{\mathbf{u}}(k|k) \dots \dots \dots (13)$$

In the case of a step-shaped control sequence, the minimization of this index (Eq. 13) is performed by using the condition

$$\hat{\mathbf{u}}(k+j|k) = \mathbf{u}(k); \quad j = 1, \dots, \lambda - 1 \dots \dots \dots (14)$$

By using Eqs. 1, 2, and 14 the process output predicted at instant  $k$  for consecutive instants  $k+j$  ( $j = 1, \dots, \lambda$ ) can be expressed as a function of the current state vector  $\mathbf{x}(k)$  and the control vector  $\mathbf{u}(k)$  as follows:

$$\hat{\mathbf{y}}(k+j|k) = \mathbf{HT}(j)\mathbf{x}(k) + \mathbf{HZ}(j)\mathbf{u}(k) \dots \dots \dots (15)$$

where  $\mathbf{T}(j)$  and  $\mathbf{Z}(j)$  are matrices given by

$$\mathbf{T}(j) = \mathbf{A}^j \dots \dots \dots (16a)$$

$$\mathbf{Z}(j) = (\mathbf{I} + \mathbf{A} + \mathbf{A}^2 + \dots + \mathbf{A}^{j-1})\mathbf{B} \dots \dots \dots (16b)$$

By substituting Eq. 15 into Eq. 13 one has

$$J = \frac{1}{2} \sum_{j=1}^{\lambda} [\mathbf{HT}(j)\mathbf{x}(k) + \mathbf{HZ}(j)\mathbf{u}(k) - \mathbf{y}_r(k+j)]^T \mathbf{Q}(j) \cdot [\mathbf{HT}(j)\mathbf{x}(k) + \mathbf{HZ}(j)\mathbf{u}(k) - \mathbf{y}_r(k+j)] + \frac{1}{2} \mathbf{u}(k)^T \mathbf{R} \mathbf{u}(k) \dots \dots \dots (17)$$

Since  $\mathbf{u}(k)$  is the only unknown in Eq. 17, it can be obtained by imposing the following condition on the gradient of  $J$ :

$$\frac{\partial J}{\partial \mathbf{u}(k)} = \mathbf{0} \dots \dots \dots (18)$$

The application of condition 18 to Eq. 17 results in

$$\alpha\mathbf{x}(k) + \beta\mathbf{u}(k) = \boldsymbol{\mu}(k) \dots \dots \dots (19)$$

where  $\alpha$  and  $\beta$  are matrices given by

$$\alpha = \sum_{j=1}^{\lambda} Z^T(j)H^TQ(j)HT(j) \dots \dots \dots (20a)$$

$$\beta = \sum_{j=1}^{\lambda} Z^T(j)H^TQ(j)HZ(j) + R \dots \dots \dots (20b)$$

and  $\mu(k)$  is a vector defined by

$$\mu(k) = \sum_{j=1}^{\lambda} Z^T(j)H^TQ(j)y_r(k + j) \dots \dots \dots (21)$$

which represents a weighted average of the reference trajectory in  $[k, k + \lambda]$ . The control vector is finally deduced from Eq. 19, resulting in the following control law:

$$u(k) = -\beta^{-1}\alpha x(k) + \beta^{-1}\mu(k) \dots \dots \dots (22)$$

The computation of the gain matrix  $\beta^{-1}\alpha$  in the control law (Eq. 22) is significantly more economic than that of the gain matrix in the optimal control law (Eq. 12), which requires the solution of the Riccati equation (Eq. 10). A particular choice of weighting matrices  $Q(j)$  and  $R$  which further simplifies the computation of matrices  $\alpha$  and  $\beta$  is

$$R = O; \quad Q(j) = O; \quad j = 1, \dots, \lambda - 1; \quad Q(\lambda) = Q \dots \dots \dots (23)$$

In this case the control law reduces to

$$u(k) = -\beta^{-1}\alpha x(k) + \beta^{-1}\gamma y_r(k + \lambda) \dots \dots \dots (24)$$

where now

$$\alpha = Z^T(\lambda)H^TQHT(\lambda) \dots \dots \dots (25a)$$

$$\beta = Z^T(\lambda)H^TQHZ(\lambda) \dots \dots \dots (25b)$$

$$\gamma = Z^T(\lambda)H^TQ \dots \dots \dots (25c)$$

From this particular choice of matrices  $Q(j)$  and  $R$ , Eq. 16 reduces to

$$J = \frac{1}{2} [\hat{y}(k + \lambda|k) - y_r(k + \lambda)]^T Q [\hat{y}(k + \lambda|k) - y_r(k + \lambda)] \dots \dots \dots (26)$$

The minimization of this index implies that the desired output at instant  $k + \lambda$  will be as close as possible to the reference trajectory. In that special case in which the input and output vectors have the same dimensions, the minimum value for  $J$  is zero. This case means imposing the criterion that the desired output at instant  $k + \lambda$  should have a given value  $y_r(k + \lambda)$ , which appears as a simple generalization for  $\lambda > 1$  of the predictive control law used in some previous papers (Martín-Sánchez 1976; Rodellar and Barba 1985) in which  $\lambda$  was considered equal to 1.

#### DIGITAL CONTROL OF STRUCTURES

Consider an  $n$ -DOF model of a structure subjected to a dynamic load. Its motion can be described by the equation

Register for free at <https://www.scipedia.com> to download the version without the watermark

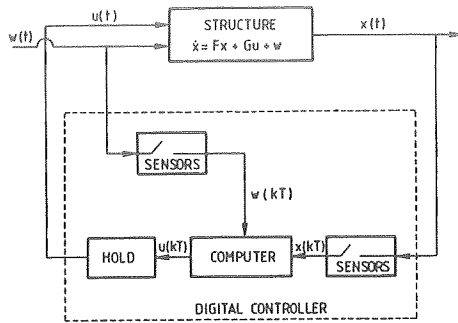


FIG. 2.—Closed-Loop Digital Control Scheme

$$M\ddot{d} + C\dot{d} + Kd = f + g \dots \dots \dots (27)$$

where  $M$ ,  $C$ , and  $K$  = the  $n \times n$  mass, the damping, and the stiffness matrices, respectively;  $d$ ,  $\dot{d}$ , and  $\ddot{d}$  = the displacement, velocity, and acceleration  $n$  vectors relative to the ground, respectively;  $f$  = an  $n$  force vector induced by the external excitation; and  $g$  = the  $n$  control force vector whose component  $g_j$  is the control force applied in the horizontal direction by an actuator on the  $j$ th degree of freedom. If the number of actuators is  $r \leq n$ , it can be written as

$$g = Lu \dots \dots \dots (28)$$

where  $u$  = an  $r$  control vector whose components are the forces supplied by the actuators; and  $L$  is an  $n \times r$  matrix whose elements are equal either to zero or to one, depending on the presence or absence of an actuator on the different degrees of freedom.

By defining a  $2n$  state vector  $x^T = [d^T, \dot{d}^T]$  and using Eq. 28, Eq. 27 can be written in the form

$$\dot{x} = Fx + Gu + w \dots \dots \dots (29)$$

where

$$F = \begin{bmatrix} 0 & I \\ -M^{-1}K & -M^{-1}C \end{bmatrix}; \quad G = \begin{bmatrix} 0 \\ M^{-1}L \end{bmatrix}; \quad w = \begin{bmatrix} 0 \\ M^{-1}f \end{bmatrix} \dots \dots \dots (30)$$

Since the closed-loop control of the structure is governed by a computer, the digital control scheme shown in Fig. 2 can be considered. At each sampling instant  $k$ , sensors are used to measure the displacement and velocity components of the state vector  $x(kT)$ , where  $T$  = the sampling period. Another sensor can be used to measure the dynamic load that defines the excitation vector  $w(kT)$ . The digital computer calculates the value for the control vector  $u(kT)$  by means of a given algorithm. A hold device keeps constant the value of the  $u(kT)$  constant between  $kT$  and  $kT + T$  thus converting the sequence of vectors  $u(kT)$  into a continuous time control signal  $u(t)$ , which is applied to the structure by means actuators. If a linear variation of the excitation  $w(t)$  is assumed between  $kT$  and  $kT + T$ , the following discrete-time model describing the diagram of Fig. 2 can be formulated (Modellar and Barbat 1985a; 1985c):

$$\begin{aligned}
 \mathbf{x}(kT + T) &= \mathbf{A}\mathbf{x}(kT) + \mathbf{B}\mathbf{u}(kT) \\
 &+ \mathbf{P}_1\mathbf{w}(kT + T) + \mathbf{P}_2[\mathbf{w}(kT + T) - \mathbf{w}(kT)] \dots \dots \dots (31)
 \end{aligned}$$

where  $\mathbf{A}$ ,  $\mathbf{P}_1$ , and  $\mathbf{P}_2 = 2n \times 2n$  matrices and  $\mathbf{B}$  a  $2n \times r$  matrix defined by

$$\mathbf{A} = e^{\mathbf{F}T}; \quad \mathbf{B} = \mathbf{P}_1\mathbf{G} \dots \dots \dots (32a)$$

$$\mathbf{P}_1 = \int_0^T e^{\mathbf{F}\mu}d\mu; \quad \mathbf{P}_2 = -\frac{1}{T} \int_0^T e^{\mathbf{F}\mu}\mu d\mu \dots \dots \dots (32b)$$

The discrete-time output (or response variables) to be controlled can be represented by an  $m$  vector  $\mathbf{y}(kT)$  expressed as

$$\mathbf{y}(kT) = \mathbf{H}\mathbf{x}(kT) \dots \dots \dots (33)$$

where  $\mathbf{H}$  is the  $m \times 2n$  output matrix.

### COMPARATIVE EXAMPLES AND ANALYSIS

**Example 1.**—Consider a 1 DOF system with mass  $m = 866.5 \times 10^3$  kg, stiffness  $k = 128 \times 10^6$  N/m, and damping  $c = 346.6 \times 10^3$  kg/s subjected to the horizontal seismic ground acceleration  $a(t)$  shown in Fig. 3. The system's equation of motion takes the form of Eq. 27, where the excitation is  $f = -ma(t)$ . The discrete-time Eqs. 31 and 33 have been used to simulate this system, the output matrix being  $\mathbf{H} = (1, 0)$ . In order to perform the digital control of the system, both optimal and predictive control methods have been applied with a sampling period  $T = 0.5$  sec.

For the implementation of optimal control, Eq. 10 should be used. However, if the number  $N$  of steps becomes large,  $\mathbf{P}(j)$  reaches a steady-state  $\mathbf{P}_s$ , which verifies the algebraic equation

$$\mathbf{P}_s = \mathbf{H}^T\mathbf{Q}\mathbf{H} + \Delta^T\mathbf{P}_s[\mathbf{I} + \mathbf{B}\mathbf{R}^{-1}\mathbf{B}\mathbf{P}_s]^{-1}\mathbf{A} \dots \dots \dots (34)$$

which, according to Eq. 11, leads to a constant gain matrix given by

$$\mathbf{D}_s = \mathbf{R}^{-1}\mathbf{B}^T(\mathbf{A}^T)^{-1}[\mathbf{P}_s - \mathbf{H}^T\mathbf{Q}\mathbf{H}] \dots \dots \dots (35)$$

Thus, the control law (Eq. 12) becomes

$$\mathbf{u}(j) = -\mathbf{D}_s\mathbf{x}(j) \dots \dots \dots (36)$$

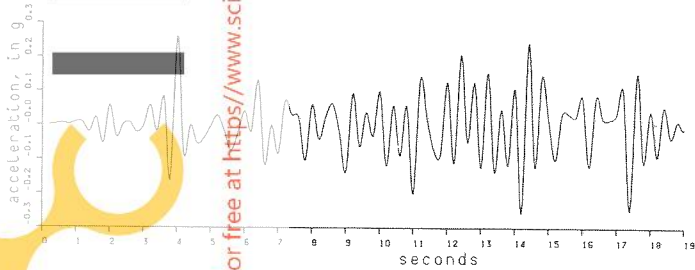


FIG. 3. Seismic Ground Acceleration



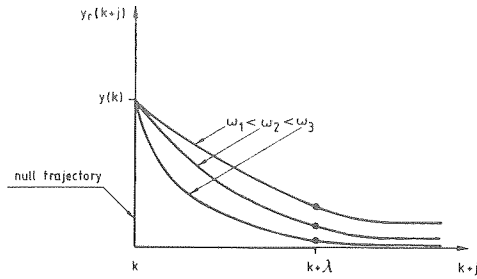


FIG. 4.—Reference Trajectories

Eq. 34 has been solved by iterating Eq. 10 until the steady-state  $P_s$  has been reached.

In this 1 DOF case, the weighting matrices reduce to positive scalars  $q$  and  $r$ . The latter has been fixed with a value  $r = 1$ , while  $q$  is the parameter needed to choose in each application.

Predictive control has been implemented by using the control law (Eq. 24). The value  $y_r(k + \lambda)$  is selected belonging to a reference trajectory defined by the discrete-time equation

$$y_r(k + j) = \theta_1 y_r(k + j - 1) + \theta_2 y_r(k + j - 2); \quad j = 1, \dots, \lambda \dots \dots \dots (37a)$$

which is redefined at instant  $k$  starting from the present and previous values of the system's response, i.e.

$$y_r(k) = y(k); \quad y_r(k - 1) = y(k - 1) \dots \dots \dots (37b)$$

Parameters  $\theta_1$  and  $\theta_2$  have been chosen in such a way that Eq. 37a represents the free response of a harmonic oscillator, with a critical damping and a certain frequency  $\omega$  with the initial conditions of Eq. 37b. As shown in Fig. 4, a faster trajectory corresponds to a higher frequency. In a limit case, a null trajectory may be considered, thus resulting in a discontinuous jump from  $y(k)$  to a null value. The weighting matrix  $Q$  reduces, in this 1 DOF case, to a positive scalar fixed equal to 1. Consequently the parameters to be chosen in each application are the value of  $\lambda$  defining the prediction horizon and that of frequency  $\omega$  of the reference trajectory.

Numerical experiments have been carried out in which the optimal control has been applied by varying the parameter  $q$  and the predictive control has been used by varying the value of  $\lambda$  for different values of  $\omega$ . Fig. 5 shows a summary of the results obtained. In Figs. 5(a) and 5(b) the rms and the maximum value for the displacement response are shown for both the optimal and the predictive control methods respectively. Similar plots are presented in Figs. 5(c) and 5(d) for the control forces. In the case without control, the maximum and rms of the displacement response were 9.7 cm and 3.1 cm, respectively. As can be seen in Figs. 5(a) and 5(b), the displacements under optimal control reduce as the weighting parameter  $q$  increases, while at the same time the control forces in Figs. 5(c) and 5(d) increase. In the predictive control case, it can be observed in the same figures that, for a given reference trajectory, the

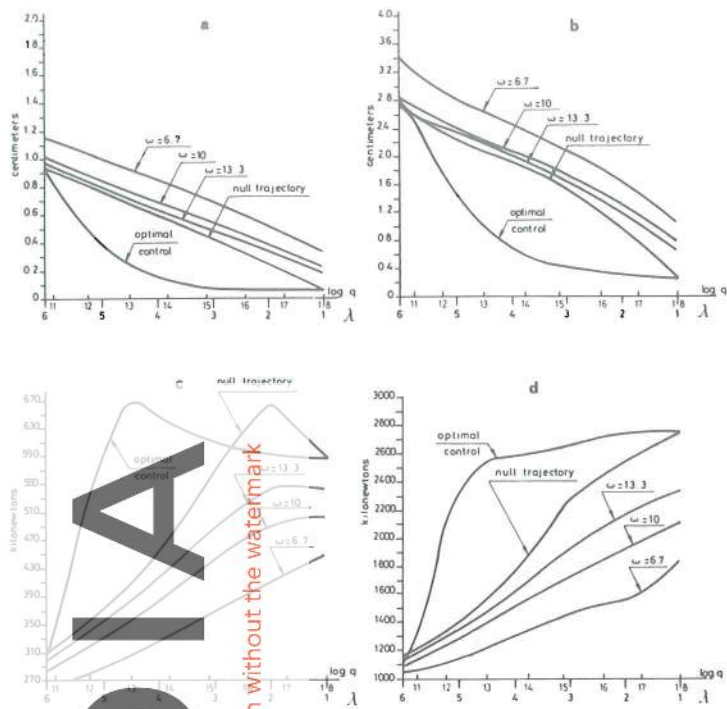


FIG. 5.—Optimal and Predictive Control Experiments: (a) Root Mean Square Displacement; (b) Maximum Displacement; (c) Root Mean Square Control Force; and (d) Maximum Control Force

decrease in parameter  $\lambda$  results in a decrease in the displacements, together with an increase in the control forces. At the same time, by comparing the graphs for different reference trajectories, it can be seen that, for a greater  $\omega$ , displacements are smaller and control forces are greater. These comments may be interpreted according to the physical significance of parameters  $q$  for the optimal control and  $\lambda$  and  $\omega$  for the predictive control. An increase in the value of  $q$  imposes a more demanding control since the displacement is more weighted in the performance index. A smaller value for  $q$  implies a shorter prediction horizon and, according to the strategy of predictive control, it determines a desired output closer to the equilibrium position. On the other hand, as shown in Fig. 4, a higher value for  $\lambda$  results in a faster reference trajectory, which also imposes a desired output closer to equilibrium. Consequently, the smaller the value for  $\lambda$  or the greater the value of  $\omega$ , the more demanding is the control action. Finally, it can be noted that the effect of increasing  $q$  in optimal control is similar to that of reducing the value for  $\lambda$  or increasing the value for  $\omega$ . Furthermore, it can be concluded that for a given value of  $q$  there are a couple of values  $\lambda - \omega$  for which optimal and predictive control produce similar results.

Example 2.—In order to perform a comparison between optimal and predictive control methods in a more complex case, the 10 DOF shear

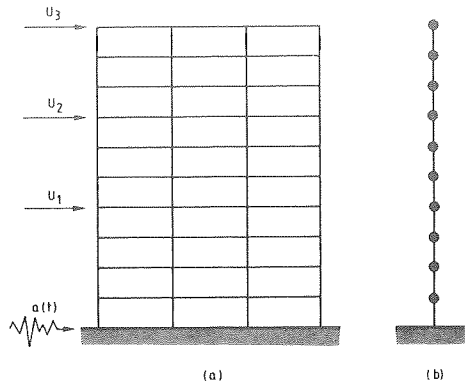


FIG. 6.—(a) Building Structure; (b) Lumped Mass Model

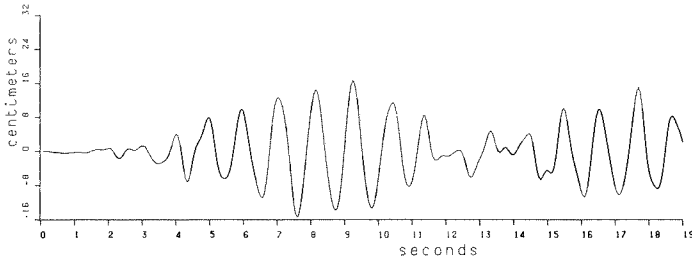
building model shown in Fig. 6 has been considered. It is subjected to the ground acceleration  $a(t)$  of Fig. 3. Its horizontal motion is described by Eq. 27 with  $f = -Mia(t)$ ,  $i$  being the identity vector. The values for the mass and stiffness characteristics are given in Table 1. The damping matrix  $C$  corresponds to a damping ratio of 0.05 for each mode of vibration and was calculated by using a direct modal evaluation procedure (Wilson and Penzien 1972). In order to simulate the response of the controlled system, the discrete-time Eqs. 31 and 33 have been used. The output  $y(kT)$  is a 10 vector whose components are the displacements of each floor. The control action is supplied by three actuators located in floors 4, 7, and 10, respectively. This control action is then represented by a 3 control vector  $u(kT)$ . The sampling period for digital control was  $T = 0.05$  sec.

Eqs. 34–36 have been used to implement the optimal control. In this case, the weighting matrix  $R$  was fixed as equal to the  $3 \times 3$  identity matrix while  $Q = q \cdot I$ , where  $I$  = the  $10 \times 10$  identity matrix; and  $q$  = a positive scalar that is the parameter to choose in each application.

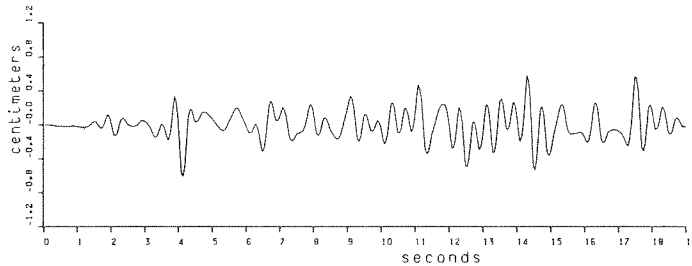
The control law of Eq. 24 has been used to apply the predictive control

TABLE 1.—Mass and Stiffness Characteristics of Structure

Floor (1)	Mass (kg) (2)	Stiffness (N/m) (3)
1	136,000	187,000,000
2	122,000	175,000,000
3	109,000	149,000,000
4	109,000	127,000,000
5	98,000	93,000,000
6	85,000	81,000,000
7	85,000	65,000,000
8	73,500	61,500,000
9	73,500	51,000,000
10	67,500	45,000,000



**FIG. 7.—Uncontrolled Displacement Response**



**FIG. 8.—Displacement Response under Optimal Control**

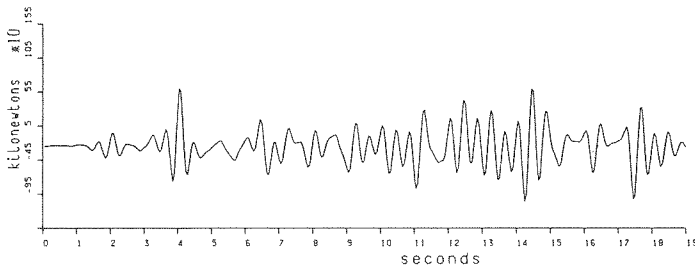


**FIG. 9.—Control Force under Optimal Control**

method.  $\mathbf{y}_r(k + \lambda)$  is, in this case, a 10 vector selected corresponding to ten scalar trajectories, one for each DOF, defined by Eqs. 37. As in the case of Example 1, all these trajectories have been defined by critical damping and frequency  $\omega$ . The weighting matrix  $\mathbf{Q}$  has been fixed as equal to the  $10 \times 10$  identity matrix. Thus the application of control law (Eq. 24) finally requires the choice of only parameters  $\lambda$  and  $\omega$ .

Several experiments have been simulated in which optimal and predictive control have been applied with different values for their parameters. Some time histories are given in Figs. 7–11 for floor 10. Fig. 7 shows the uncontrolled displacement. Figs. 8 and 9 show the displacement and the control force for the optimal control applied with  $q = 10^{12}$ , while Figs. 10 and 11 show them for the predictive control applied with

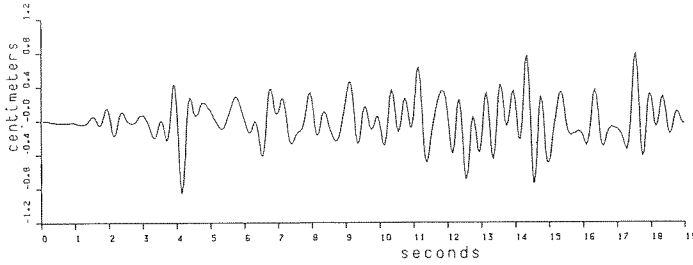


FIG. 10.—Displacement Response under Predictive Control

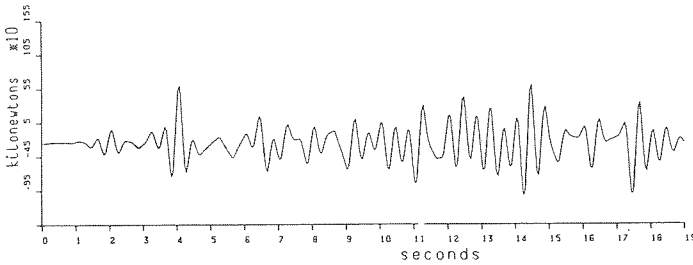


FIG. 11.—Control Force under Predictive Control

$\lambda = 2$  and a null reference trajectory.

By comparing the results in Figs. 8–11, it can be observed that the values for the displacements and the control forces are similar and represent a significant reduction of the structural response, as compared with the uncontrolled one, with reasonable control forces. This conclusion is in agreement with the results obtained in Example 1.

However, some advantages of the predictive control should be pointed out. First, the computation of the gain matrix  $\beta^{-1}\alpha$  in the predictive control law (Eq. 24) is significantly more economical than the calculation of gain matrix  $D_s$  in the optimal control law (Eq. 36), which needs the recursive solution of the Riccati equation (Eq. 34). As an example, in the case of the 10-DOF structure, 40 iterations have been required to obtain the steady-state Riccati matrix. Thus the computation of  $D_s$  has taken 24.2 sec, while the computation of the gain matrix  $\beta^{-1}\alpha$  has taken 0.53 sec by using a VAX-750 computer. Moreover, the fact that the predictive control strategy redefines a prediction horizon at each sampling instant allows the development of a predictive controller, which is especially useful for structural control. Thus a control algorithm has been formulated in Rodellar and Barbat (1985) that uses the on-line measurement of the excitation signal. An algorithm that considers pulse control forces has also been developed in Barbat, et al. (1986) within the driver block solution based on shaped control sequences. Finally, the redefinition of the control problem at each sampling instant permits an updating of the parameters by means of an estimation algorithm (Martín-Sánchez 1980; Martín-Sánchez and Shah 1984). This adaptive capability may be useful for the control of structures with nonlinear behavior.

## CONCLUSIONS

This paper has presented a general formulation of the predictive control method, which has been applied for structural control. A comparison between optimal and predictive control has been carried out.

Predictive control may be well suited to structural control for the following reasons:

1. It is mathematically simple and easy to use through a digital computer. It does not require the solution of a Riccati equation as does the optimal control method.
2. Its effectiveness in reducing the structural response is equivalent to that of optimal control.
3. It can incorporate practical aspects such as the use of pulse control forces, the use of the on-line measured excitation for computing the control forces, as well as the use of an adaptive algorithm in order to handle structures with nonlinear behavior.

## APPENDIX I.—REFERENCES

- Abdel-Rohman, M., and Leipholz, H. H. (1978). "Structural control by pole assignment method." *J. Engrg. Mech. Div.*, ASCE, 104(5), 1159–1175.
- Abdel-Rohman, M., and Leipholz, H. H. (1979). "A General approach to active structural control." *J. Engrg. Mech. Div.*, ASCE, 105(6), 1007–1023.
- Barbat, A. H., Rodellar, J., and Martín-Sánchez, J. M. (1986). "Pulse control of the earthquake response of elevated water tanks." *Proc. 8th European Conf. Earthquake Engrg.*, Lisbon, Portugal, 5, 8.5/49–8.5/56.
- Brogan, W. L. (1974). *Modern control theory*. Prentice Hall, New York, N.Y.
- Bryson, A. E., and Ho, Y. C. (1975). *Applied optimal control*. Hemisphere Publ. Corp., Washington, D.C.
- Chang, J., and Soong, T. T. (1980). "Structural control using active tuned mass dampers." *J. Engrg. Mech. Div.*, ASCE, 106(6), 1091–1098.
- Martin, C. R., and Soong, T. T. (1976). "Modal control of multistory structures." *J. Engrg. Mech. Div.*, ASCE, 102(4), 613–623.
- Martín-Sánchez, J. M. (1974). "Contribution to model reference adaptive systems from hyperstability theory," thesis submitted to the Universidad Politécnica de Cataluña, Barcelona, Spain, in partial fulfillment of the requirements for the degree of Doctor of Philosophy (in Spanish).
- Martín-Sánchez, J. M. (1976a). "A new solution to adaptive control." *Proc. of IEEE*, 64(8), 1209–1218.
- Martín-Sánchez, J. M. (1976b). "Adaptive-predictive control method." *USA Patent No. 4, 197, 576*.
- Martín-Sánchez, J. M. (1977). *Modern control theory; adaptive-predictive control method: Theory and applications*. March Foundation of Spain, Madrid, Spain (in Spanish).
- Martín-Sánchez, J. M. (1980). "Adaptive-predictive control system (C.I.P.)." *European Patent Application No. 811026210-2206*.
- Martín-Sánchez, J. M., and Shah, S. L. (1984). "Multivariable adaptive-predictive control of a binary distillation column." *Automatica*, 20(5), 607–620.
- Meirovitch, L., and Silverberg, L. M. (1983). "Control of structures subjected to seismic excitation." *J. Engrg. Mech. Div.*, ASCE, 109(2), 604–618.
- Rodellar, J. (1982). "Optimal design of driver block in the adaptive-predictive control system," thesis presented to the Universidad de Barcelona, Barcelona, Spain, in partial fulfillment of the requirements for the degree of Doctor of Philosophy (in Spanish).
- Rodellar, J., and Barbat, A. H. (1985a). "Numerical analysis of the seismic response: A state space approach." *Proc. Numerical Methods in Engineering: Theory*

- and Applications, A. A. Balkema, Boston, Mass., 273–279.
- Rodellar, J., and Barbat, A. H. (1985b). "Digital control of structures subjected to seismic actions." *Proc. Numerical Methods in Engineering: Theory and Applications*, A. A. Balkema, Boston, Mass., 281–290.
- Rodellar, J., and Barbat, A. H. (1985c). "Active control of building structures under measured seismic loads." *Engrg. Computations*, 2(2), 128–134.
- Rodellar, J., and Martín-Sánchez, J. M. (1986). "Predictive structural control," in *Active Control II*, H. H. Leipholz, Ed., North Holland, New York, N.Y.
- Roorda, J. (1980). "Experiments in feedback control of structures." in *Structural Control*, H. H. Leipholz, Ed., North-Holland, New York, N.Y., 629–662.
- Sage, A. P., and White, C. C. (1977). *Optimum system control*. Prentice-Hall Inc., Englewood Cliffs, N.J.
- Wilson, E. L., and Penzien, J. (1972). "Evaluation of orthogonal damping matrices." *Int. J. Num. Met. Engrg.*, 4, 5–10.
- Yang, J. N. (1975). "Application of optimal control theory to civil engineering structures." *J. Engrg. Mech. Div.*, ASCE, 101(6), 819–838.
- Yang, J. N., and Giannopoulos, F. (1978). "Active tendon control of structures." *J. Engrg. Mech. Div.*, ASE, 104(3), 551–568.
- Yao, J. T. P. (1972). "Concept of structural control." *J. Str. Div.*, ASCE, 98(7), 1567–1574.

## APPENDIX II.—NOTATION

The following symbols are used in this paper:

- A** = discrete-time system matrix;  
 $a(t)$  = earthquake ground acceleration;  
**B** = discrete-time control matrix;  
**C** = damping matrix;  
**D** = optimal control gain matrix;  
 $D_s$  = steady-state optimal control gain matrix;  
 $d, \dot{d}, \ddot{d}$  = displacement, velocity, and acceleration vectors;  
**F** = continuous-time system matrix;  
**f** = excitation force vector;  
**G** = continuous-time control matrix;  
**g** = control force vector;  
**H** = output matrix;  
**I** = identity matrix;  
**i** = identity vector;  
**J** = cost function;  
**j** = index indicating time instant;  
**K** = stiffness matrix;  
**k** = sampling instant;  
**L** = actuator matrix;  
**M** = mass matrix;  
**N** = optimal control final instant;  
 $P(k)$  = Riccati matrix;  
 $P_s$  = steady-state Riccati matrix;  
 $P_1, P_2$  = discrete-time excitation matrices;  
 $Q(j), Q$  = output weighting matrices;  
**q** = output weighting factor;  
 $R(j), R$  = control weighting matrices;  
**T** = sampling period;  
 $T(j)$  = matrix of prediction (Eq. 15);

$\mathbf{u}$	=	control vector;
$\mathbf{u}_0$	=	term of control law 9;
$\mathbf{u}(k + j k)$	=	sequence of control vectors;
$\mathbf{w}$	=	excitation vector;
$\mathbf{x}$	=	state vector;
$\mathbf{x}(k + j k)$	=	predicted sequence of state vectors;
$\mathbf{y}$	=	displacement vector;
$\mathbf{y}(k + j k)$	=	predicted process output sequence;
$\mathbf{y}_d$	=	desired output;
$\mathbf{y}_r(k + j)$	=	reference trajectory;
$\mathbf{Z}(j)$	=	matrix of prediction (Eq. 15);
$\boldsymbol{\alpha}, \boldsymbol{\beta}, \boldsymbol{\gamma}$	=	matrices of the predictive control law;
$\boldsymbol{\eta}(k + j)$	=	vector sequence verifying Eqs. 5a–b;
$\theta_1, \theta_2$	=	parameters of the reference trajectory;
$\lambda$	=	length of the prediction horizon;
$\boldsymbol{\mu}(k)$	=	weighted average of the reference trajectory; and
$\omega$	=	frequency of the reference trajectory.